Geomechanics and Engineering, *Vol. 41, No. 1 (2025) 103-114*
https://doi.org/10.12989/gae.2025.41.1.103

A numerical study on the effect of geobag connectors on the slope stability

Junwoo Shin[1a], Kyungwon Park[2b] and Boo Hyun Nam*[2]

[1]*Department of Civil Engineering, Kumoh National Institute of Technology, Gumi, Republic of Korea*
[2]*Department of Civil Engineering, College of Engineering, Kyung Hee University, Yongin, Republic of Korea*

(*Received December 7, 2024, Revised March 6, 2025, Accepted March 10, 2025*)

Abstract. Geobags are commonly used as a rapid and effective reinforcement solution for areas such as coastlines and slopes, typically installed in a stacked configuration. In certain cases, geobag connectors are employed to enhance binding strength. However, there is limited research on the applicability and performance of these connectors. This study investigates the effects of geobag connectors on reinforced slopes, focusing on their applicability and performance. To evaluate the influence of geobag connectors, scenarios were developed considering factors such as slope angle, rainfall exposure, and the presence or absence of connectors. A coupled stress-seepage analysis was performed to assess the safety factor of geobag-reinforced slopes and the stresses experienced by the connectors before, during, and after rainfall events. The results indicated that, across all scenarios, slope safety factors decreased with rising water levels due to high rainfall intensity. A slight increase in the safety factor was observed when connectors were applied. However, the stress generated at the interface at the steepest front angle, when the water level rises due to rainfall, was significantly different from that observed under dry conditions. On the other hand, the difference in stress was minimal, regardless of the rise in water level at the gentlest front angle. Through these results, it was confirmed that the reinforcing effect of the geobag connector diminished as the front angle became less steep. This highlights the necessity for further analysis regarding the applicability of the geobag connector in relation to various influencing factors.

Keywords: geobag connector; geobag reinforced slope; limit equilibrium method; strength reduction method

1. Introduction

Geobags are commonly employed as a protective measure to prevent soil erosion along coastlines and riverbanks. In the ecological advantages, the characteristics of the lightweight and portable material allow for effective construction in both large- and small-scale projects, leading them a economical and sustainable method for protecting coastlines, riverbanks, and mountain region. A number of studies have been conducted to assess the effectiveness of geobag, which is comparable with effectiveness of geogrid (Kang *et al*. 2015, Hou *et al*. 2023, 2024). Recio *et al*. (2019) developed an analytical stability formula that elucidates the impact of geobag deformation on the slip and overturn stability of coastal structures. Khajenoori *et al*. (2021) conducted a full-scale experiment to assess the hydraulic stability of geobag embankments utilized for riverbank protection and reported their findings. Li *et al*. (2023) designed and constructed a sandbag for coastal protection, comparing its performance with existing protective measures. Guin *et al*. (2024) presented an optimal design for geobag embankments based on river flow conditions and evaluated their performance.

In addition, geobags are promoted by their cost-effectiveness and ease of construction, making them suitable for use on slopes where the access to construction equipment or materials is limited. A number studies investigated the use of geobag as structures and systems. Rahardjo *et al*. (2017, 2018, 2019, 2020, 2022) introduced the GeoBarrier System as a retaining wall alternative to traditional concrete walls. Liu *et al*. (2019) demonstrated the applicability of geobags as construction materials by building retaining walls with soilbags filled with clay. Sadr *et al*. (2022) employed a numerical analysis approach to investigate the performance of soilbags used as columns. Wu *et al*. (2020) analyzed the performance of a geobag wall system incorporating recycled concrete aggregates using the Discrete Element Method (DEM). Zhou *et al*. (2018) examined the penetration and stability performance of geobags as a slope protection measure for agricultural land drainage channels through experimental methods. Most studies on geobags with application of slope reinforcement have employed either a geogrid-mixed method, a general stacking method, or a geosynthetics-reinforced slope technique (Vahedifard *et al*. 2016, Zhang *et al*. 2023, Yazdani *et al*. 2023). The construction of geobags is typically classified into various types, including horizontal stacking, vertical stacking, and mixed stacking, depending on the stacking technique used.

The geobag containing vegetation substantially reinforce the slope of soil by augmenting shear strength and providing stabilization against landslides via root systems that improve soil cohesion and friction angle, though the effectiveness varies based on root distribution, mechanical properties, and species traits (Sonnenberg *et al*. 2010, Veylon *et al*. 2015). Vegetation contributes to the reduction

*Corresponding author, Professor
E-mail: boohyun.nam@khu.ac.kr
[a]Ph.D. Student
[b]Ph.D. Student

ISSN: 2005-307X (Print), 2092-6219 (Online)

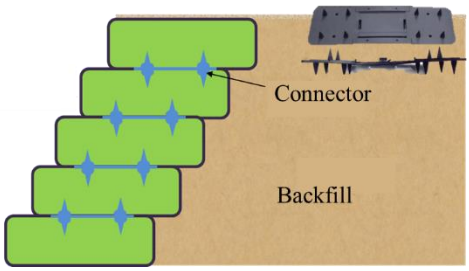

(a) Schematic diagram of Geobag-reinforced slope

(b) Geobag-reinforced slope

Fig. 1 Construction site of geobag-reinforced slope

of soil water content, hence improving shear strength, however the reinforcement provided by roots may be less than certain model estimates (Xie *et al*. 2020). The incorporation of geobags with vegetation offers an eco-friendly and cost-effective alternative to traditional slope stabilization methods (Wu 2013, Wang *et al*. 2023).

Recently, the geobag connectors have been introduced. When geobags are constructed using the stacking method, the bonding strength can be inadequate, making them susceptible to damage from rain or other external forces, furthermore, the recent occurrence of extreme weather events has raised concerns about the reliability of the reinforcing effects of geobags. Thus, the geobag has a great potential to enhance bonding strength between two vertical geobags. However, the studies on the performance of the geobag connector is limited and only a few studies are available. Shin *et al*. (2019) analyzed the dynamic behavior of a retaining wall composed of geobags and geobag connectors through large-scale shaking table experiments and numerical analysis.

The presenting study investigates the performance of the geobag-connector reinforced slope via a series of finite-element (FE) based numerical analyses. The study aimed at identifying the factors that affect the slope stability and to analyze the safety factor and stress behavior of the connector to evaluate the applicability, limitations, and performance of the geobag connector. Seepage analysis that accounts for water infiltration due to rainfall events was employed, and shear strength reduction (SRM) method was employed to quantitatively determine the stability change due to rainfall events.

2. Background on the geobag connector

The geobag connector is effective in enhancing the structural integrity and interlocking between two vertical geobags. This effect is distinguishable under high stacked geobag slope and under dynamic loadings such as seismic activity. Constructed from resilient materials, geobag connectors enhance durability and strength, improving the overall effectiveness of geobag installations. The effectiveness of the connector for slope stabilization was studied under severe environment (Mohri *et al*. 2009, Rahardjo *et al*. 2020). The geobag connector is generally made by weather-resistant materials such as PE (Polyethylene) and PP (Polypropylene) which are able to withstand severe environmental conditions such as UV exposure, moisture, and mechanical wear.

The connectors, mainly composed of polyvinyl chloride (PVC) and polypropylene (PP) materials, have the spikes so that it is tightly interlocked when installed between two geobags in a vertical manner. The standard size of the geobag connectors is generally 300-450 mm in length and 100 mm ±10 mm in width. There are different types of the geobag connectors that have different features such as shape, strength, and spike number. For example, Type D connector, shown in Fig. 1(a), has the spike with a plastic board drain (PBD) system and the spike height of 1.5 cm. For the construction and installation of geobags and geobag connector, it is necessary to follow the specific procedure for ensuring optimal construction, inducing slope stabilization and management. First, the site is prepared by organizing and compacting ground to create stable foundation for the geobag slope. Using field material such as sand or gravel in the site, geobag is filled with designed weight to consistent densities. Subsequently, the geobag is stacked with a certain pattern until a target height, and compaction work is conducted to reach to the target density. The connectors are strategically placed between layers of geobags to interlock them, enhancing the structural integrity of the assembly. The example of the geobag reinforced slope is shown in Fig. 1(b).

3. Numerical modeling

3.1 Methodology and scope

Numerical analysis was conducted to evaluate the effect of the geobag connector on the stability of geobag-reinforced slopes. The procedure of numerical analysis, as shown in Fig. 2, includes characterization of material properties, identification of the influencing factors to slope stability, unsaturated infiltration analysis, and slope stability analysis. The slope analysis was based on the results of the infiltration analysis.

To identify the factors affecting slope stability, we approached the issue by categorizing both internal and external factors. Here, internal factors refer to controllable factors, whereas external factors pertain to uncontrollable factors that arise from natural phenomena. For the internal

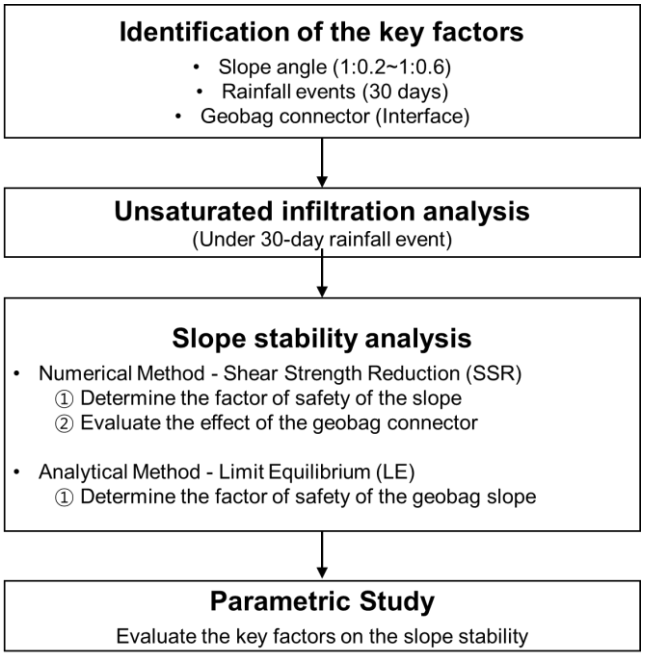

Fig. 2 Flow chart for numerical analysis of slope stability analysis

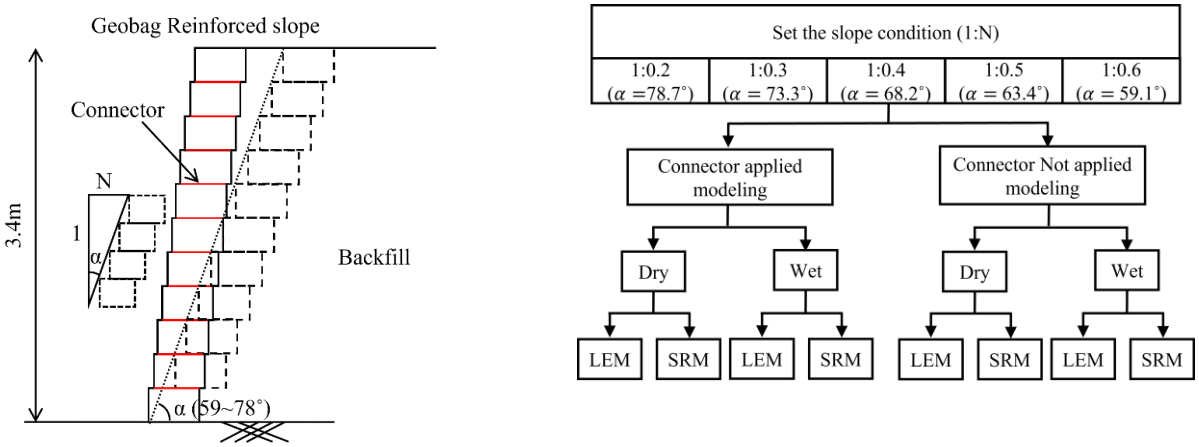

(a) Modeling geometry (b) Analysis cases with different scenarios

Fig. 3 Modeling details of the slope stability analysis

factor, we focused on the slope angle. The slope angle of the geobag-reinforced slope was selected as a key consideration because it can be controlled during the initial design stage, and mechanical instability of the slope can be induced by variations in the slope angle. For the external factor, we focused on the fluctuations in water levels resulting from exposure to rainfall. One common mechanism of failure in general structures or soil is attributed to the reduction in strength characteristics and the increase in earth pressure resulting from rising water levels. Furthermore, previous studies have demonstrated that rainfall infiltration decreases slope stability (Gasmo *et al*. 2000, Huang *et al*. 2009, rahardjo *et al*. 2010, Tang *et al*. 2018, Wang *et al*. 2020). A recent study analyzed the correlation between stability analysis and displacement in relation to rainfall intensity, rainfall duration, slope angle, and soil type (Yu *et al*. 2023).

Therefore, we identified the key factors influencing slope stability that the slope angle and fluctuating in water levels resulting from rainfall. We developed various scenarios by integrating these selected factors. Fig. 3 shows the geometry of the slope and the flow chart summarizing the different scenarios of the numerical analysis.

The unsaturated infiltration analysis was conducted to observe changes in the water level. Depending on the consideration of the rainfall events, which is associated with unsaturated infiltration analysis, it is classified as ‘Dry’ or ‘Wet’.

For significant fluctuations in water levels, the annual rainfall during periods of heavy precipitation was utilized. In addition, the impact of connectors on slope stability due to fluctuations in water levels was analyzed. The slope angle of the geobag-reinforced slope was modeled with ratios ranging from 1:0.2(78.7°) to 1:0.6(59.1°), as

Table 1 Material properties used in the FE model (Jangwon engineering co., ltd. 2010, Park *et al*. 2018)

Samples	Elastic modulus (MPa)	Poisson`s ratio	Unit weight (kN/m^3)	Cohesion (kPa)	Internal friction angle (˚)	Permeability coefficient (m/day)
Geobag	24	0.3	16.9	15.51	28.97	0.0194
Backfill	30	0.3	16.9	8.33	30.54	0.0238
Weathered soil	36.5	0.33	13.1	7.0	27.0	0.163
Weathered rock	117.85	0.3	20.0	3.0	35.0	6.04e-06
Soft rock	305.5	0.31	22	7	40	5.23e-08

Table 2. Material properties of the connector interface used in the FE model (from Shin *et al*. 2018, Park *et al*. 2018)

Material	Normal Stiffness (kN/m^3)	Shear Stiffness (kN/m^3)	Cohesion (kPa)	Internal friction angle (˚)
Connector (Interface)	7000.0	3500.0	8.0	15.0

illustrated in Fig. 3(a). Based on this modeling, the impact of the geobag connector on the slope angle was analyzed. The analysis case was established using the influencing factors outlined in the process depicted in Fig. 3(b).

Slope stability analysis was conducted using the SRM and the Limit Equilibrium Method (LEM). The maximum shear strain was analyzed using SRM to estimate a reasonable virtual failure surface. In addition, the stability of the geobag-reinforced slope was investigated by considering different scenarios of the influencing factors. The stability obtained by SRM was compared with the stability by LEM.

3.2 Model geometry

The finite element (FE) method utilized in this study is a two-dimensional plane strain model. Fig. 4 shows the modeling details. Based on the slope height (H) of 3.4 m, the model geometry is extended to a width of 5H and a height of 4H. The slope is composed of total 17 geobag units. Two vertical geobags are reinforced by the connectors that link them together. In the rear side of the slope, a couple of geobags were placed for waterways not for reinforcement.

For accurate and cost-effective penetration analysis, the mesh size was modeled to be as small and square as possible.

3.3 Material properties

A typical soil profile in the mountain area of Incheon-si was used and the soil profile includes is multi-layered, comprising backfill, weathered soil, weathered rock, and soft rock. The backfill soil (or geobag filler) are usually obtained using weathered residual soil sourced from the surrounding area. The relative compaction of 83% was assigned. The constitutive model used in this study is Mohr-Coulomb model. Table 1 shows the material properties utilized in the numerical analysis.

Geobag connectors was used to enhance both friction and bonding roles between two vertical geobags. Consequently, the geobag connector was modeled as an interface element. A couple of studies modeled the geobag interface, without the connector, in a similar way (Shin *et al*. 2018, Nguyen *et al*. 2023). Since the geobag connector was used in this study, materials properties of the interface are higher than the geobag itself. A series of direct shear test were performed to evaluate the shearing performance of the geobag and the geobag connector (Park *et al*. 2018). The shearing resistance was then compared for the geobag alone and geobag with connector, and with varied material properties, a number of numerical simulations were conducted to match the measured and computed behaviors for the connector-reinforced geobag. When both measured and computed results are well matched, the material properties of the connector interface were determined as final input value. Table 2 presents the mechanical properties of the geobag connector as an interface element, including vertical and shear stiffness coefficients, cohesion, and the internal friction angle.

3.4 Unsaturated infiltration analysis

The rainfall conditions were based on the intense heavy rainfall that occurred in South Korea from May 1 to July 31, 2017. One month (July) was selected during this period and applied to the surface, as illustrated in Fig. 5.

The pore water pressure at the ground surface was set to not exceed zero to prevent ponding. Considering that the infiltration target ground consists of the same material (weathered soil), the negative pore water pressure was set to 5 kPa, based on the findings of McCarthy's research (McCarthy 1982). The unsaturated properties function for weathered soil and backfill, used in unsaturated infiltration analysis, has been obtained (see Fig. 6).

The infiltration analysis was conducted daily, resulting in the determination of the water level for the month of July. The stability of the Geobag-reinforced slope was analyzed

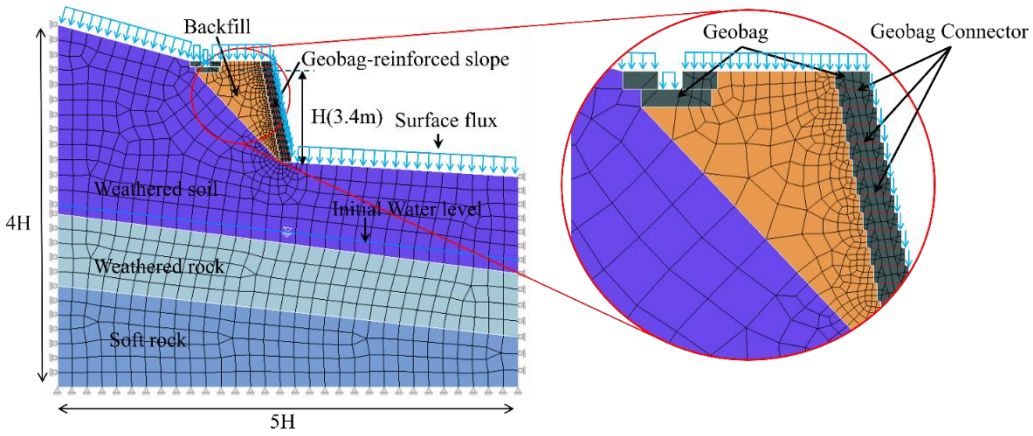

Fig. 4 Schematic diagram of Geobag-reinforced slope numerical model

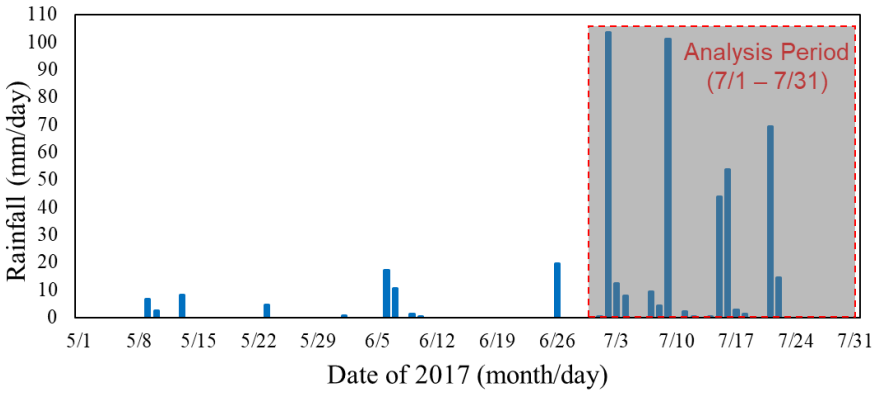

Fig. 5 Rainfall records analyzed in this study (1st July 2017-31th July 2017)

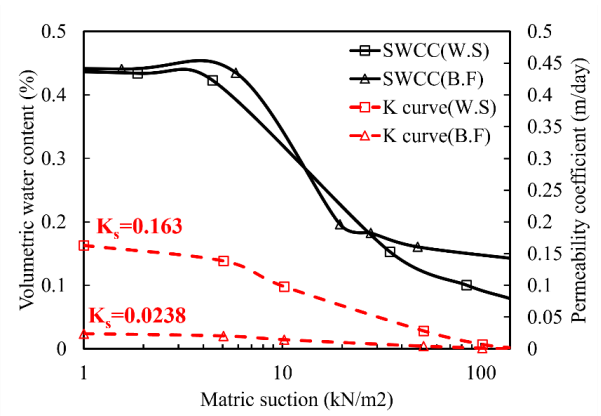

Fig. 6 Unsaturated properties function used in this study

by conducting SRM and LEM analyses, incorporating the water level for each date in the modeling process.

4. Results of the numerical analysis

4.1 Seepage analysis

The infiltration analysis consists of a total of 32 stages, which are corresponded to time in day. In the initial stage, a steady-flow analysis was conducted on the groundwater level using the initial water level. Later, from Day 2 through Day 32, the water infiltration analysis along with unsaturated soil mechanic was conducted.

For the result check, the steepest slope angle of 1:0.2(78.7°) was examined as a representative cross-section (see Fig. 7). To determine the highest water level resulting from the infiltration analysis over the course of a month, we checked the water levels on the days of the maximum rainfall occurred each week during the entire month. The

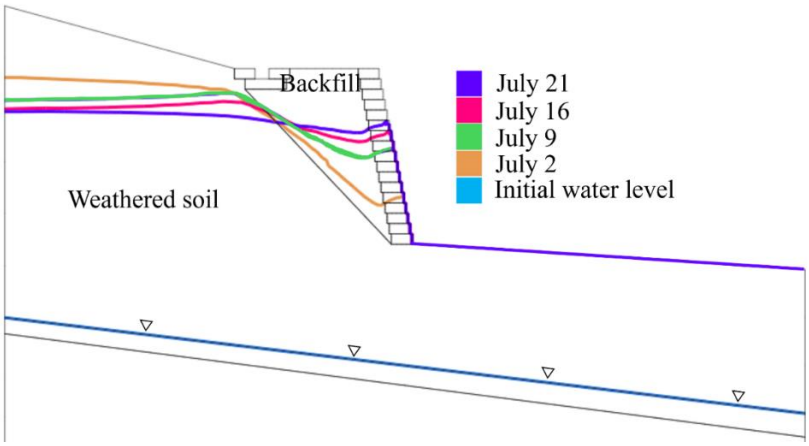

Fig. 7 Water level change according to unsaturated seepage analysis

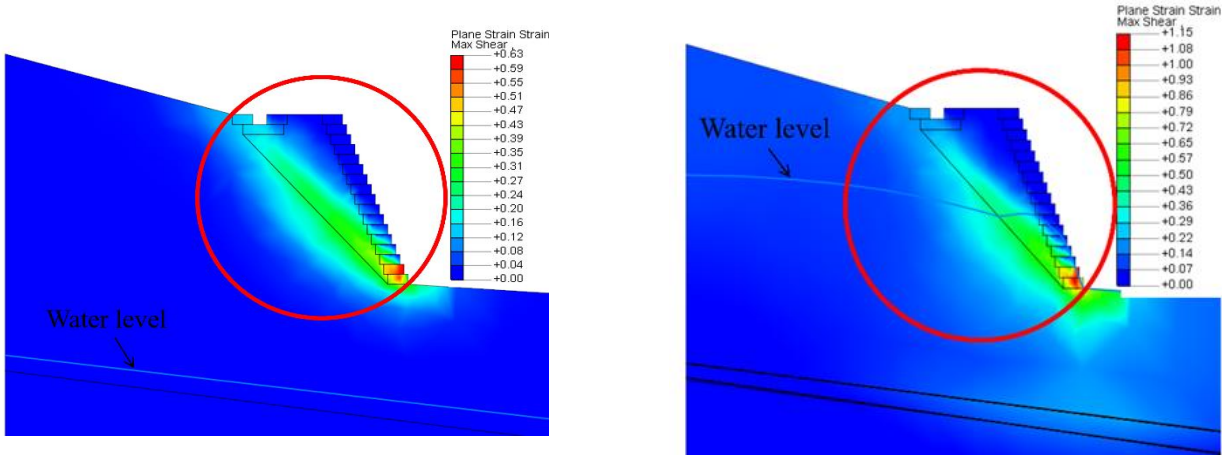

(a) Maximum shear strain at initial water level (b) Maximum shear strain at maximum rainfall

Fig. 8 Maximum shear strain of geobag-reinforced slope according to water infiltration

dates of maximum weekly rainfall were July 2, July 9, July 16, and July 21. Fig. 7 shows the water levels for those selected dates. As times goes, with the consideration of rainfall events, the water level in the backfill decreases while it increases in the backfill, and ultimately similar water levels. On July 2, the water level reaches its maximum in the weathered soil, while it remained lowest in the backfill. On July 9, the water level is lower in the weathered soil but higher in the backfill than that of July 2. As time goes over the next following days, the water level decreases in the weathered soil but increases in the backfill. On July 21, the water levels of the weathered soil and the backfill became comparable, with the backfill exhibiting the highest water level. It was confirmed that the changes in water levels exhibited the same pattern across all slope angles.

4.2 Slope stability analysis

The slope stability analysis in this study employed both the LEM and the SRM. The LEM is a method that considers the ground as a single soil body and analyzes stability by considering the equilibrium condition of the force or moment for the virtual failure surface. The slice method was examined to facilitate calculations of the soil mass along the assumed failure surface. The representative slice methods include Bishop, Fellenius, Spencer, and Janbu. According to a recent study, the Fellenius method likely underestimate stability in sandy slopes (Doan *et al*. 2023). Therefore, this study utilized the Bishop method, which is relatively fast and accurate. The LEM is characterized by assuming a virtual failure surface. The stability is computed only based on the assumed failure surface and the geometry is not modeled as a mesh; thus, the modeling of geobag connectors is not allowed. Thus, the LEM method was used to compare the stability results obtained by SRM when the geobag connectors are not used.

The SRM is one of the FE methods and the analysis is performed until the point where the constitutive equation does not converge by reducing the soil properties c and Φ and considers that point as failure. This approach facilitates the easy induction of failure. Inducing failure also allows for the estimation of a realistic failure surface. This result was used to inform the virtual failure surface in the LEM. Taking these factors into account, the SRM was applied to analyze the influence of the geobag connector on the stability of the geobag-reinforced slope. First, to estimate

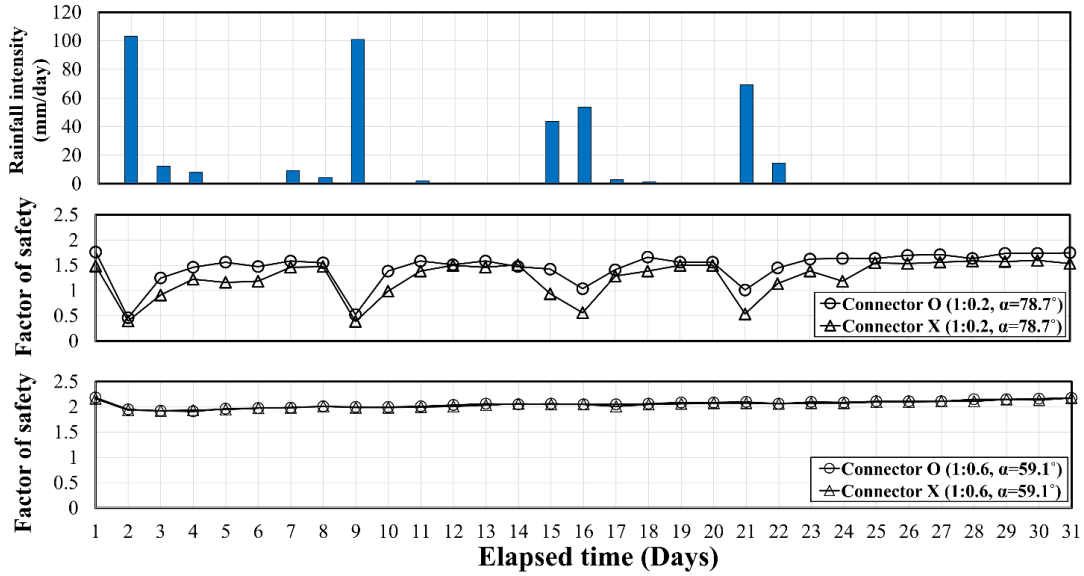

(a) SRM

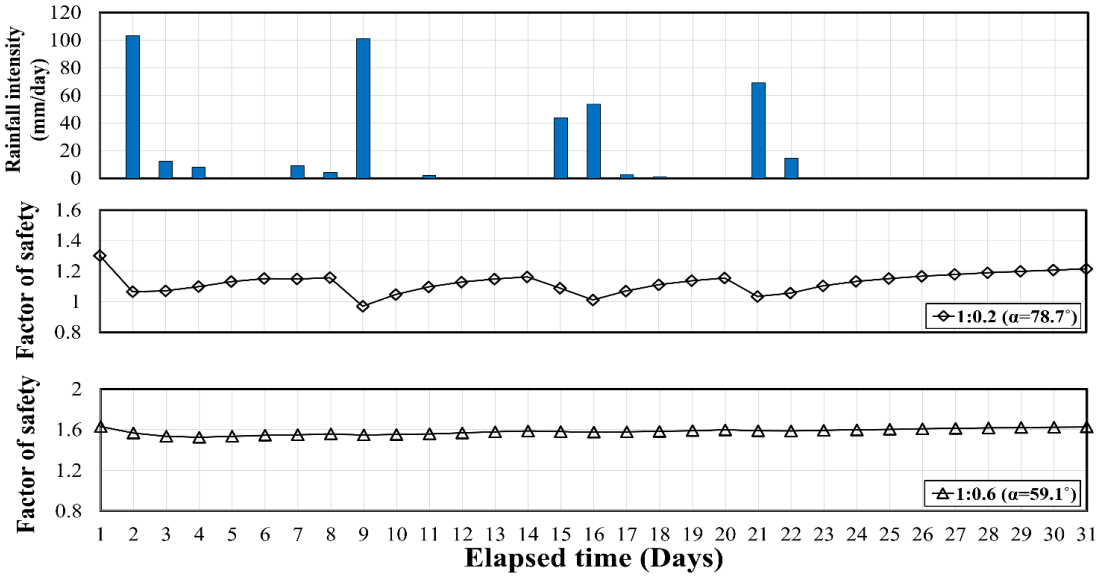

(b) LEM

Fig. 9 Safety factor of slope according to fluctuation water level due to rainfall exposure

the virtual failure surface through the SRM analysis, the maximum shear strain was analyzed for all analysis cases considering the slope angle and water level change. The analysis was conducted for the Dry and Wet seasons (the day when the water level was the highest) for all slopes. The analysis revealed that the maximum shear strain consistently occurred at the interface between the weathered soil and backfill across all cases. Fig. 8 shows the example of SRM result, exhibiting the maxim shear strain at both initial and maximum water levels. This result indicates a reasonable failure surface, attributed to the reduction of soil properties; thus; the virtual failure surface was defined as a circular failure along the backfill layer.

4.2.1 Effect of the geobag connector along with water level (rainfall events)

First of all, the stability of the slope was evaluated in relation to water-level fluctuations (see Fig. 7) caused by rainfall exposure. The stability of the slope was then assessed by varying the slope angle, which is an internal factor. The combination of the two influencing factors were then assessed. The analysis results compared the steepest slope (1:0.2, 78.7°) with the gentlest slope (1:0.6, 59.1°), which showed the most significant differences in results. The results of slope stability analysis using the LEM and the SRM are presented in Figs. 9(a) and 9(b), respectively.

According to the LEM analysis results, the safety factor of the slope, at the steepest slope, varied due to the water-level fluctuations caused by rainfall exposure. In particular, the safety factor sharply decreased on days with maximum weekly rainfall. In contrast, at the gentlest slope, the changes in the safety factor due to water level fluctuations from rainfall exposure were minimal. This result indicates that the impact of water-level fluctuations on the safety

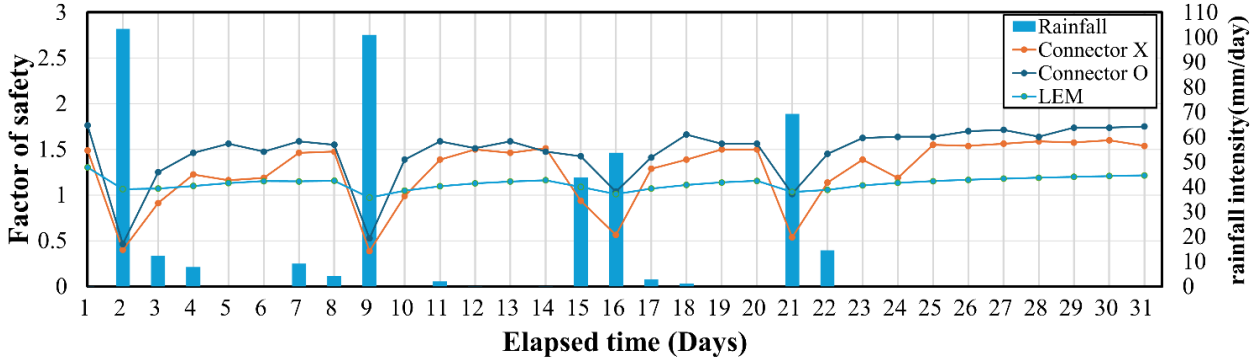

(a) 1:0.2(78.7˚)

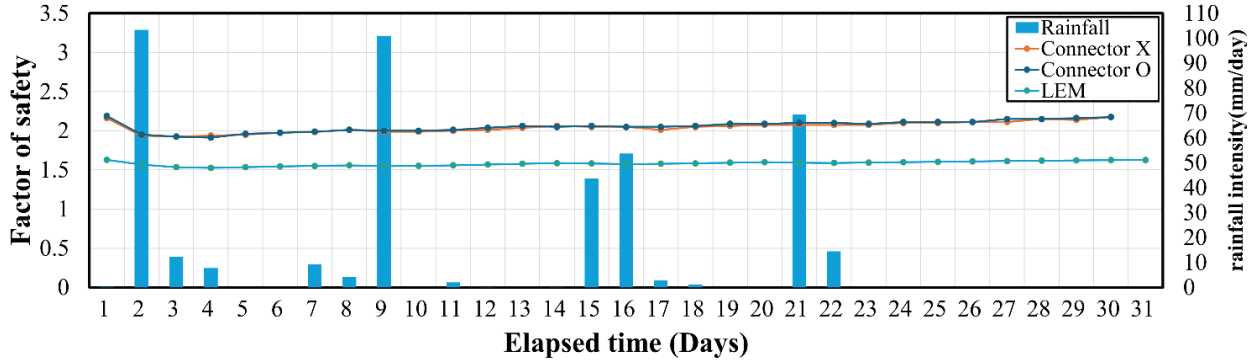

(b)1:0.6(59.1˚)

Fig. 10 Safety factor of the slope according to rainfall exposure by interpretation method

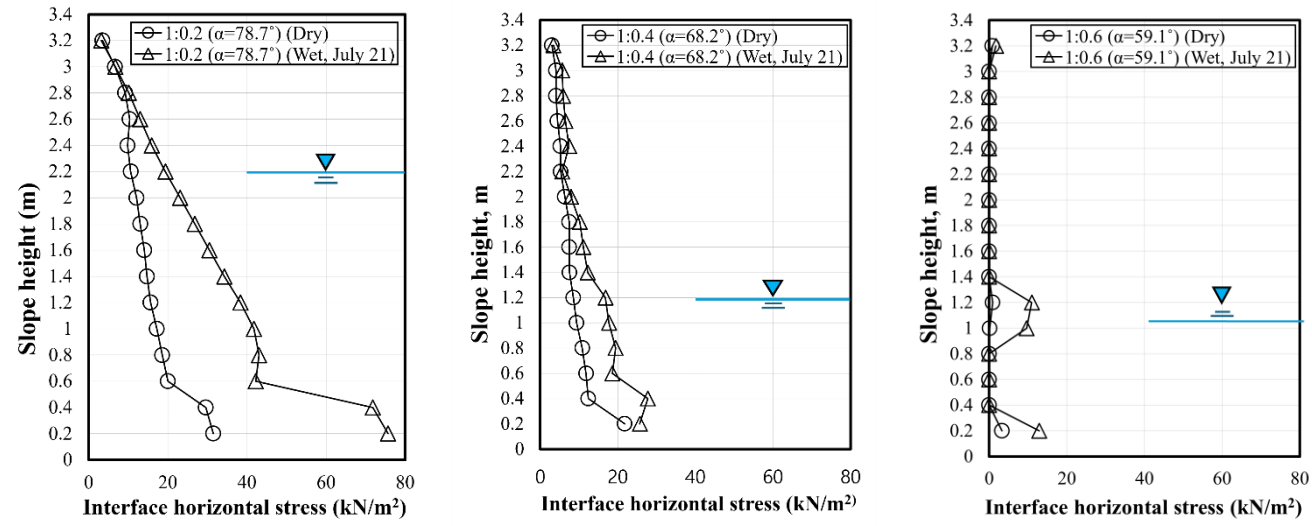

(a) 1:0.2(78.7˚) (b) 1:0.4(68.2˚) (c) 1:0.6(59.1˚)

Fig. 11 Horizontal stress behavior in connectors due to water level rise caused by exposure to rainfall

factor significantly varies with the slope angle.

According to the SRM analysis, the safety factor of the slope, at the steepest angle, experienced a sharp decline on the day of maximum weekly rainfall. This behavior was also observed in the analysis using the LEM. Additionally, similar behavior was observed regardless of the application of connectors. However, when connectors were applied, a relatively higher safety factor was observed. In contrast, the change in the safety factor of the slope due to water level fluctuations from rainfall exposure at the gentlest angle was minimal.

Subsequently, the results of SRM and LEM were then compared over time Fig. 10 shows the effect of rainfall events on the slope stability using the two analysis methods. It is observed that on the day of maximum weekly rainfall, the SRM yields a lower safety factor, whereas at other

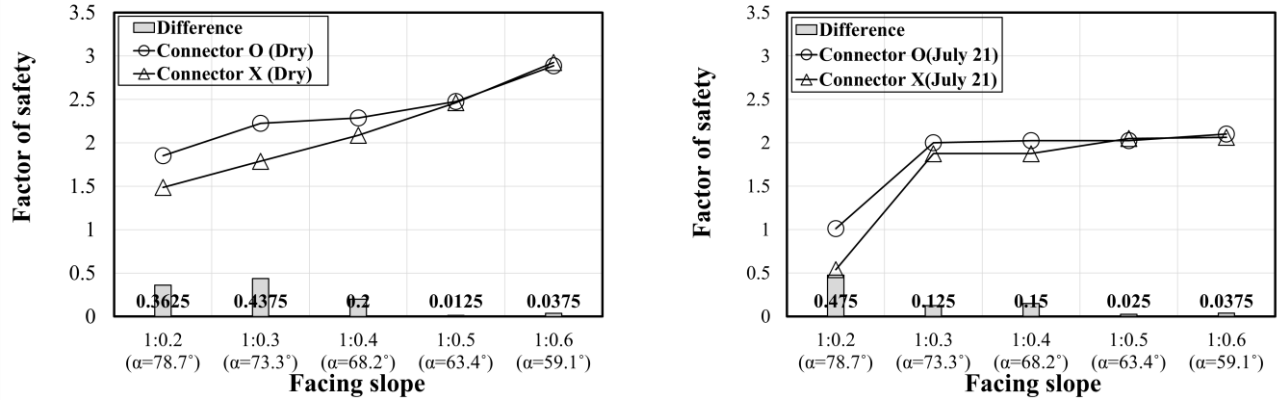

(a) SRM (Dry) (b) SRM (Wet, July 21)

Fig. 12 Trend of slope safety factor for varied slope angle

times, it indicates a higher safety factor. These results can be understood through the characteristics of the two interpretation methods. The LEM is a simple analytical method used to evaluate the stability of local failure surfaces. This method can either underestimate or overestimate the safety factor depending on the failure surface assumed. On the other hand, the SRM is a method that analyzes the entire geometry by discretizing it and reducing the shear strength parameters, c and Φ, applied to the soil layers; thus this method may underestimate the safety factor depending on the consideration of external factors. Nevertheless, both analysis methods show a tendency for the safety factor to decrease due to water level fluctuations caused by rainfall exposure, particularly on the steepest slopes. In the gentlest slopes, there was a tendency for the safety factor to remain almost unchanged regardless of water level fluctuations, strength reduction, or the presence of connectors. In summary, the analysis of these results indicates that water level fluctuations due to rainfall exposure affect slope stability. Additionally, it showed that the impact of water level fluctuations caused by rainfall exposure significantly decreases depending on the slope angle.

Lastly, we conducted a comparative analysis of the horizontal stress occurring in the connector under Dry and Wet conditions (maximum water level due to rainfall exposure). To illustrate the trends resulting from water level fluctuations, Fig. 11 presents the results of three cases: the steepest, moderate, gentlest slopes. It is observed that significant level of stress occurs in the connector under Wet condition. In particular, the difference between Wet and Dry conditions becomes evident as the slope steepens. Additionally, in all cases, there is a sharp increase in the stress on the connector at a slope height of 0.4 m. This indicates the location where the maximum shear strain occurs, as shown in Fig. 7. Ultimately, it can be concluded that the maximum shear strain leads to the maximum interfacial stress in the connector.

4.2.2 Effect of the geobag connector along with slope angle

The stability of the slope was then analyzed considering the varied slope angle. Additionally, we applied changes in water level, due to external factors such as rainfall exposure, to assess the stability of the slope based on the combination of these two influencing factors. The interpretation results compared the “Dry” condition and “Wet” condition (with the highest water level on July 21). The results of the slope stability analysis, based on the LEM and SRM, are presented in Fig. 12.

Firstly, we evaluated the safety factor of the slope based on the presence or absence of connectors and varied slope angle under Dry condition. Generally, the less steep the slope is, the lower level of the driving force by the soil block takes place, making the slope more stable. The interpretation results also indicate that regardless of the presence of connectors, as the slope becomes gentler, the safety factor tends to increase or converge (see Fig. 12(a)).

Up to a slope angle of 1:0.4(68.2°), a minimum reinforcement effect of 0.2(78.7°) in safety factor was observed. From a slope angle of 1:0.5(63.4°), the reinforcement effect was found to be very minimal in a safety factor. This result indicates that under dry conditions, as the slope angle becomes gentler, the reinforcement effect of the connector may be negligible. However, it was found that the safety factor did not meet the required safety standard.

Secondly, we evaluated the safety factor of the slope based on the presence or absence of connectors and varied slope angle under Wet condition. The analysis results showed that in cases where connectors were applied, there was no change in the safety factor from a certain slope angle. In contrast, when connectors were not applied, the safety factor tended to increase as the slope angle became gentler (see Fig. 12(b)). It is noteworthy that in cases where connectors were applied, a clear reinforcement effect was observed at the steepest angle, with a difference of 0.475 in the safety factor. From an angle of 1:0.3(73.3°), it was observed that when connectors were applied, there was no reinforcement effect, and the safety factor tended to converge. These results suggest that under wet conditions, the reinforcement effect is lower compared to dry conditions, indicating that the rise in water levels caused by rainfall exposure may limit the connectors' effectiveness.

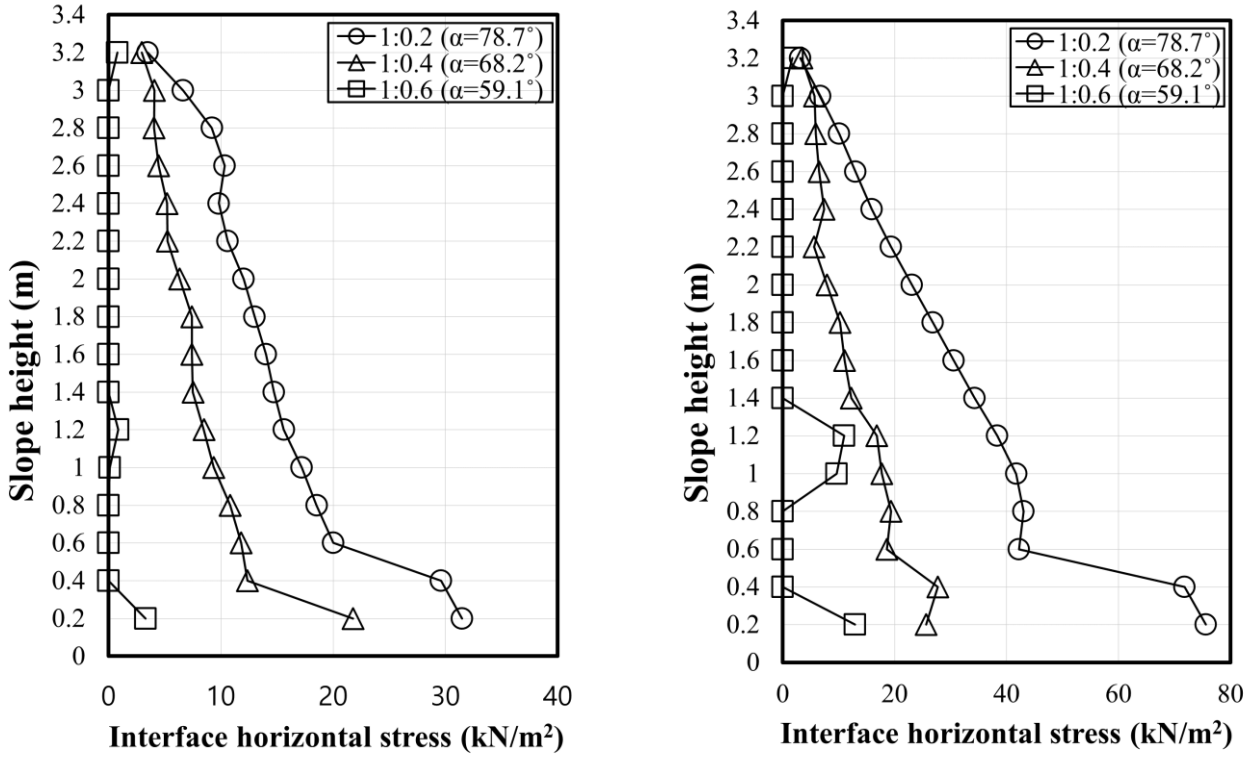

(a) SRM (Dry) (b) SRM (Wet, July 21)

Fig. 13 Trend of slope safety factor, when the connector is employed, for varied slope angle

Lastly, we analyzed the horizontal stress on the connector based on the slope angle. To illustrate the trends according to the slope angle, we compared the steepest slope, moderate slope, and gentlest slope under Dry and Wet conditions, as shown in Fig. 13. The condition is the day with the highest water level. It was indicated that as the slope angle becomes steeper under Dry condition, the horizontal stress on the connector increases. This observation can also be seen in Wet condition. Additionally, when comparing the connector stress between wet and dry conditions at the steepest slope, it can be noted that there is more than a twofold difference. This suggests that as the soil mass on the slope becomes saturated, the unit weight increases, leading to greater activity and significantly higher resistance in the connector.

5. Discussion

This study carried out the slope stability analysis for the slope reinforced by the geobag connector, particularly, the numerical analysis was employed to quantitatively evaluate the effect of the connector along with water level and slope angle on the stability factor. According to the results, as the slope angle becomes steeper, the safety factor decreases (see Fig. 12). For those steep slopes with relatively low safety factors, the effect of the geobag connector is obvious, indicating the increased safety factors. For the steepest slope (slope angle of 78.7°) in the analysis, the connector increases the safety factor by approximately 0.5. On the other hand, when the slope angle becomes less stiff, the positive effect of the connector diminished, and for the slope angles less than 63.4° , the connector does not play a role any further. Therefore, the critical angle is 63.4° for the use of geobag connector, which means that the connector is not effective for the slope angle less than 63.4. Of course, depending on site condition and environment (e.g., rainfall, water level, etc.) the critical angle may be somewhat varied. This critical value may be useful for the design of the geobag connector reinforced slope.

6. Conclusions

In this study, the effectiveness of the geobag connector was evaluated using a numerical method, which is finite element (FE) based. First, the SRM method was employed to determine the stability of the slope with no connector, and the results were compared with LEM analysis. Subsequently, the effects of affecting factors, such as geobag connector, water-level fluctuation, and slope angle, on the geobag reinforced slope were investigated in term of slope stability factor. Followings are conclusions driven from a series of numerical analyses. The following are the conclusions derived from a series of analysis results.

• As expected, the safety factor of the slope tends to decrease as the slope angle become steeper and the water level increases; however, as the slope angle become gentle, there are cases where the water-level change does not affect

the safety factor of the slope. This suggests that there is an effective range of influence of the influence factors on the stability of the slope depending on the interaction between the influence factors.

• When the connectors are applied, its reinforcement effect exhibits a nonlinear relationship with the slope angle. When the slope angle is the steepest, the reinforcement effect is clear regardless of the dry or rainy condition. However, as the slope angle become gentle, there are cases where the safety factor is not affected in spite of the connector reinforcement. This indicates that the reinforcement effect of the connector is also significantly influenced by various factors.

• In summary, if the slope angle does not exceed the critical value, the water-level change is not the main influence factor on the stability of the slope, and the reinforcement of the connector is also ineffective. Ultimately, this implies that there exists a critical value that impacts the safety factor, which is contingent upon the interaction of these influencing factors. This highlights the necessity for further research on the applicability of the connector in relation to various influencing factors. The threshold value for the slope angle was determined to be 1:0.5(63.4°).

Acknowledgments

This work was supported by the National Research Foundation of Korea(NRF) grant funded by the Korea government(MSIT)(RS-2025-00516147).

References

Chua, Y.S., Rahardjo, H. and Satyanaga, A. (2022), "Structured soil mixture for solving deformation issue in GeoBarrier System", *Transport. Geotech.*, **33**, 100727. https://doi.org/10.1016/j.trgeo.2022.100727.

Doan, N.S. (2023), "Reliability analysis and uncertainty quantification of clay and sand slopes stability evaluated by Fellenius and Bishop's simplified methods", *Int. J. Geo-Eng.*, **14**(1), 22. https://doi.org/10.1186/s40703-023-00200-2.

Gasmo, J.M., Rahardjo, H. and Leong, E.C. (2000), "Infiltration effects on stability of a residual soil slope", *Comput. Geotech.*, **26**(2), 145-165. https://doi.org/10.1016/S0266-352X(99)00035-X.

Guin, S. and Bhattacherjee, D. (2024), "Applicability of geobags as a sustainable riverbank protection measure", *Indian Geotech. J.*, 1-14. https://doi.org/10.1007/s40098-024-00895-9.

Hong-In, P., Takahashi, A. and Likitlersuang, S. (2024), "Engineering and environmental assessment of soilbag-based slope stabilisation for sustainable landslide mitigation in mountainous area", *J. Environ. Management*, **359**, 120970. https://doi.org/10.1016/j.jenvman.2024.120970.

Hou, J., Chu, C.X., Li, J.Z., Copeland, T., Chen, J. and Nam, B.H. (2024), "An analytical model of horizontal-vertical geogrid reinforced foundation", *KSCE J. Civil Eng.*, **28**, 2673-2680. https://doi.org/10.1007/s12205-024-0354-7.

Hou, J., Liu, S., Nam, B. and Ma, Y. (2023), "Bearing capacity and mechanism of the H–V geogrid-reinforced foundation", *Polymers*, **15**, 2606. https://doi.org/10.3390/polym15122606.

Huang, M. and Jia, C.Q. (2009), "Strength reduction FEM in stability analysis of soil slopes subjected to transient unsaturated seepage", *Comput. Geotech.*, **36**(1-2), 93-101. https://doi.org/10.1016/j.compgeo.2008.03.006.

Kang, Y., Nam, B., Zornberg, J.G. and Cho, Y.H. (2015), "Pullout resistance of geogrid reinforcement with in-plane drainage capacity in cohesive soil", *KSCE J. Civil Eng.*, **19**, 602-610. https://doi.org/10.1007/s12205-013-0274-4.

Jangwon Engineering Co., Ltd. (2010), "Geotechnical investigation report for dongchun 1 district urban development project", Technical Report, Jangwon Engineering Co., Ltd., Korea.

Khajenoori, L., Wright, G. and Crapper, M. (2021), "Laboratory investigation of geobag revetment performance in rivers", *Geosciences*, **11**(8), 304. https://doi.org/10.3390/geosciences11080304.

Kristo, C., Rahardjo, H. and Satyanaga, A. (2017), "Effect of variations in rainfall intensity on slope stability in Singapore", *International Soil and Water Conservation Research*, 5(4), 258-264. https://doi.org/10.1016/j.iswcr.2017.07.001.

Li, Y., You, Z.J., Ma, Y. and Ren, B. (2023), "Quantitative assessment of the shoreline protection performance of geotextile sandbags at an in-situ coastal experimental station", *Geotext. Geomembranes*, **51**(3), 371-380. https://doi.org/10.1016/j.geotexmem.2023.01.001.

Liu, S., Fan, K. and Xu, S. (2019), "Field study of a retaining wall constructed with clay-filled soilbags", *Geotext. Geomembranes*, **47**(1), 87-94. https://doi.org/10.1016/j.geotexmem.2018.11.001.

McCarthy, D.F. and McCarthy, D.F. (1977), *Essentials of soil mechanics and foundations (Vol. 35)*, Reston: Reston Publishing Company.

Mohri, Y., Matsushima, K., Yamazaki, S., Lohani, T.N., Tatsuoka, F. and Tanaka, T. (2009), "New direction for earth reinforcement: disaster prevention for earthfill dams", *Geosynth. Int.*, **16**(4), 246-273. https://doi.org/10.1680/gein.2009.16.4.246.

Nguyen, A.D., Nguyen, V.T. and Kim, Y.S. (2023), "Finite element analysis on dynamic behavior of sheet pile quay wall dredged and improved seaside subsoil using cement deep mixing", *Int. J. Geo-Eng.*, **14**(1), 9. https://doi.org/10.1186/s40703-023-00186-x.

Park, K.W. (2018), "Stability analysis of full scaled geobag retaining wall structure through field pilot test", M.S. Dissertation, Incheon National University, Incheon

Rahardjo, H., Gofar, N., Satyanaga, A., Leong, E.C., Wang, C.L. and Johnny Wong, L.H. (2019), "Effect of rainfall infiltration on deformation of geobarrier wall", *Geotech. Geol. Eng.*, **37**, 1383-1399. https://doi.org/10.1007/s10706-018-0693-6.

Rahardjo, H., Kim, Y., Gofar, N. and Satyanaga, A. (2020), "Analyses and design of steep slope with GeoBarrier system (GBS) under heavy rainfall", *Geotext. Geomembranes.*, **48**(2), 157-169. https://doi.org/10.1016/j.geotexmem.2019.11.010.

Rahardjo, H., Nio, A.S., Leong, E.C., and Song, N.Y. (2010), "Effects of groundwater table position and soil properties on stability of slope during rainfall", *J. Geotech. Geoenviron. Eng.*, **136**(11), 1555-1564. https://doi.org/10.1061/(ASCE)GT.1943-5606.0000385.

Recio, J. and Oumeraci, H. (2009), "Process based stability formulae for coastal structures made of geotextile sand containers", *Coast. Eng.*, **56**(5-6), 632-658. https://doi.org/10.1016/j.coastaleng.2009.01.011.

Sadr, A., Kaliakin, V.N., Hataf, N. and Manahiloh, K.N. (2022), "Numerical study of soilbag columns and comparison to encased soil columns in loose sand", *Comput. Geotech.*, **142**, 104588. https://doi.org/10.1016/j.compgeo.2021.104588.

Shin, E.C., Shin, H.S. and Park, J.J. (2019), "Numerical simulation and shaking table test of geotextile bag retaining wall structure", *Environ. Earth Sci.*, **78**(16), 507.

https://doi.org/10.1007/s12665-019-8503-x.
Sonnenberg, R., Bransby, M.F., Hallett, P.D., Bengough, A.G., Mickovski, S.B. and Davies, M.C.R. (2010), "Centrifuge modelling of soil slopes reinforced with vegetation", *Can. Geotech. J.*, **47**(12), 1415-1430. https://doi.org/10.1139/T10-037.
Tang, G., Huang, J., Sheng, D. and Sloan, S.W. (2018), "Stability analysis of unsaturated soil slopes under random rainfall patterns", *Eng. Geol.*, **245**, 322-332. https://doi.org/10.1016/j.enggeo.2018.09.013.
Thompson, A., Oberhagemann, K. and She, Y. (2020), "Geobag stability for riverbank erosion protection structures: Physical model study", *Geotext. Geomembranes*, **48**(1), 110-119. https://doi.org/10.1016/j.geotexmem.2019.103526.
Vahedifard, F., Mortezaei, K., Leshchinsky, B.A., Leshchinsky, D. and Lu, N. (2016), "Role of suction stress on service state behavior of geosynthetic-reinforced soil structures", *Transport. Geotech.*, **8**, 45-56. https://doi.org/10.1016/j.trgeo.2016.02.002.
Veylon, G., Ghestem, M., Stokes, A. and Bernard, A. (2015), "Quantification of mechanical and hydric components of soil reinforcement by plant roots", *Can. Geotech. J.*, **52**(11), 1839-1849. https://doi.org/10.1139/cgj-2014-0090.
Wang, L., Yao, Y., Li, J., Liu, K. and Wu, F. (2023), "A state-of-the-art review of organic polymer modifiers for slope eco-engineering", *Polymers*, **15**(13), 2878. https://doi.org/10.3390/polym15132878.
Wang, Y., Chai, J., Cao, J., Qin, Y., Xu, Z. and Zhang, X. (2020), "Effects of seepage on a three-layered slope and its stability analysis under rainfall conditions", *Nat. Hazards*, **102**, 1269-1278. https://doi.org/10.1007/s11069-020-03966-1.
Wu, J., El Naggar, M.H., Li, X. and Wen, H. (2020), "DEM analysis of geobag wall system filled with recycled concrete aggregate", *Constr. Build. Mater.*, **238**, 117684. https://doi.org/10.1016/j.conbuildmat.2019.117684.
Wu, T.H. (2013), "Root reinforcement of soil: review of analytical models, test results, and applications to design", *Can. Geotech. J.*, **50**(3), 259-274. https://doi.org/10.1139/cgj-2012-0160.
Xie, C., Ni, P., Xu, M., Mei, G. and Zhao, Y. (2020), "Combined measure of geometry optimization and vegetation for expansive soil slopes", *Comput. Geotech.*, **123**, 103588. https://doi.org/10.1016/j.compgeo.2020.103588.
Yazdani, H. and Ashtiani, M. (2023), "The behaviour of a strip footing resting on geosynthetics-reinforced slopes", *Geomech. Eng.*, **34**(6), 623-636. https://doi.org/10.12989/gae.2023.34.6.623.
Yu, J.Y., Woo, J.W., Kang, K.N. and Song, K.I. (2023), "Correlations between variables related to slope during rainfall and factor of safety and displacement by coupling analysis", *Geomech. Eng.*, **33**(1), 77. https://doi.org/10.12989/gae.2023.33.1.077.
Zhang, Z.L., Li, Z.W., Hou, C.T. and Pan, Q.J. (2023), "Required strength of geosynthetic-reinforced soil structures subjected to varying water levels using numeric-based kinematic analysis", *Geotext. Geomembranes*, **51**(1), 1-15. https://doi.org/10.1016/j.geotexmem.2022.08.007.